Journal of Engineering Mathematics **50:** 379–398, 2004.

Inertial effects during the infiltration of an elastic porous medium

L. MESIN* and D. AMBROSI**
*Dipartimento di Matematica, Politecnico of Torino, Corso Duca degli Abruzzi 24, 10129 Torino, Italy; *E-mail: luca.mesin@eln.polito.it; **E-mail: davide.ambrosi@polito.it*

Received 8 April 2003; accepted in revised form 14 May 2004

Abstract. This paper deals with the mathematical modeling of the coupled flow/deformation problem characterizing the industrial production of a composite material by injection moulding. The role of inertia, typically non-negligible during a short early time, is studied in terms of models of reduced complexity. Using the theory of characteristics and some considerations on the energy of the system allows one to estimate the time needed by the system to dissipate the oscillatory motion due to abrupt initial conditions.

Key words: deformable porous media, inertia, injection moulding, nonlinearity

1. Introduction

The mathematical modeling of the infiltration process of a fluid in a porous matrix subjected to a pressure gap that can yield a non-negligible deformation of the solid skeleton, is of interest in several industrial processes and environmental applications. Among others, we mention injection molding and soil consolidation. Historically the research on deformable porous media was first developed in the branch of ground-soil mechanics, soil consolidations under loading, ground-water hydrology, petroleum engineering and extraction [1, 2]. We refer to the fundamental papers by Biot [3–6]. A possible modelling framework to address this problem is the *mixture theory*: from a macroscopic point of view one writes balance equations for the solid matrix and the infiltrating fluid that at every point of the mixture are co-present, in a ratio defined by the volume fraction [7].

A simplifying assumption usually taken into account in the mathematical modeling of the infiltration process is to neglect *ab initio* the inertia of the two components. However, for injection molding processes, inertial terms affect the system in the early times, giving rise to elastic oscillations of the solid preform that rapidly decay [8].

In the present paper, under some simplifying assumptions, analytical results are obtained which can give quantitative information on inertial effects at early times of the infiltration process. The focus is on the motion of the free boundary of the solid matrix: the period and amplitude of the oscillations, and their decay rate. As a byproduct, the traveling waves in the dry (not yet infiltrated) region are also studied. All these features of the process are related to the parameters of the system: the mechanical properties of the preform (the stress-strain relation, the permeability of the matrix), the infiltrating resin and the applied pressure gap to prime the inflow process.

The paper is organized as follows:

– Section 2 is devoted to the mathematical modeling of the phenomenon, including the proper prescription of the boundary conditions;

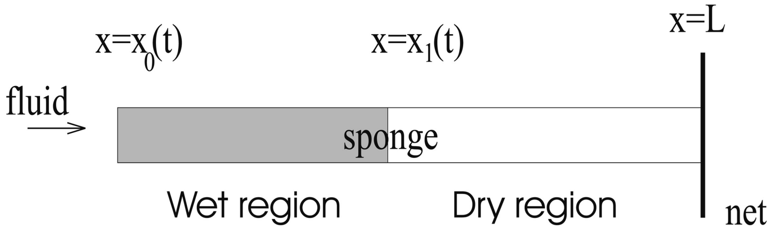

Figure 1. Representation of the one-dimensional infiltration problem. The infiltrated (wet) region is bounded by the two moving boundaries of the problem. The right border of the preform, instead, is fixed by a web, which allows only the liquid to go through.

– Section 3 gives the analytical solution of the equations, for a simple choice of the constitutive law of the stress tensor of the preform;
– in Section 4 the analytical results previously obtained are compared with numerical simulations;
– the last section gives a critical analysis of the results, suggesting directions worth of further studies.

2. The mathematical model

A possible way to address the modeling of the infiltration of a fluid into a porous medium is to adopt the mixture theory, or, more precisely, the porous media theory. The basic postulate of the theory is that the mechanical behavior of the mixture can be predicted by solving balance equations that pertain to the single components in the mixture. One can therefore state a system of balance equations for mass, momentum and possibly energy of each constituent. The assumptions that apply the general theory to the present work are isotropy of the solid preform, incompressibility of the fluid component, applicability of the Darcy's law, isothermal conditions, validity of the same stress-strain relationship in both the infiltrated region, and in the dry one.

The mathematical problem we consider intrinsically involves a moving boundary: the porous matrix (the 'sponge') deforms as far as the infiltration process advances, so that its boundary moves; the liquid infiltrates wetting the sponge and therefore the infiltration front moves with the velocity of the fluid. Air is completely neglected (for the case of a solid-liquid-air mixture, see [9]). Figure 1 shows a sketchy representation of the problem under consideration.

The following equations drive the dynamics of the two components of the mixture in the Eulerian formulation, when the inertia of the fluid is neglected:

$$\begin{aligned} &\frac{\partial \phi_s}{\partial t} + \operatorname{div}(\phi_s \mathbf{v}_s) = 0\,, \qquad &&\frac{\partial \phi_f}{\partial t} + \operatorname{div}(\phi_f \mathbf{v}_f) = 0\,, \\ &\rho_s \phi_s \frac{\mathrm{d}\mathbf{v}_s}{\mathrm{d}t} - \operatorname{div}\mathbf{T}_s = -\widehat{\mathbf{p}}_f\,, \quad &&-\operatorname{div}\mathbf{T}_f = \widehat{\mathbf{p}}_f\,, \end{aligned} \tag{2.1}$$

where ρ_s is the true mass density of the solid matrix, $\widehat{\mathbf{p}}_f$ is the momentum exchange between components due to mutual interactions, and $\mathbf{v}_\alpha$, $\mathbf{T}_\alpha$, ϕ_α are the velocity, the partial stress, the volume fractions, for the α-component, respectively. We suppose that the unsaturated region is very small when compared with the saturated one and therefore we neglect it, assuming that a sharp interface separates the wet and the dry preforms. The saturation condition reads

$\phi_s + \phi_f = 1$ and from Equations (2.1.I) and (2.1.II) we obtain that the composite velocity $\mathbf{v}_c = \phi_s \mathbf{v}_s + \phi_f \mathbf{v}_f$ is divergence-free. The following constitutive assumptions are considered

$$\widehat{\mathbf{p}}_f = P\,\mathrm{grad}(\phi_f) - \mu\phi_f^2 \mathbf{K}^{-1}(\mathbf{v}_f - \mathbf{v}_s)\,, \quad \mathbf{T}_f = -\phi_f\, P\,, \quad \mathbf{T}_s = -\phi_s\, P + \mathbf{T}\,, \tag{2.2}$$

where P is the water pore pressure, μ the viscosity of the fluid, and $\mathbf{K}$ and $\mathbf{T}$ are the permeability tensor and the excess stress of the matrix, respectively. Using these assumptions, the balance equations for the momentum of the components can be written as follows:

$$\begin{aligned} \rho_s\phi_s \frac{\mathrm{d}\mathbf{v}_s}{\mathrm{d}t} &= -\phi_s\,\mathrm{grad}\,P + \mathrm{div}\,\mathbf{T} + \mu\phi_f^2\mathbf{K}^{-1}(\mathbf{v}_f - \mathbf{v}_s)\,, \\ 0 &= -\phi_f\,\mathrm{grad}\,P - \mu\phi_f^2\mathbf{K}^{-1}(\mathbf{v}_f - \mathbf{v}_s)\,. \end{aligned} \tag{2.3}$$

Equation (2.3.II) is usually referred to as Darcy's equations.

2.1. One-dimensional infiltration and boundary conditions

The balance equations can be conveniently rewritten in Lagrangian coordinates attached to the solid component [10, Section 10.2], [11]. In the following we restrict ourselves to one-directional infiltration. In this context the composite velocity is constant, and a simple equation for the motion of the infiltration front can be recovered, [12].

It is convenient to introduce the dependent variable *void ratio* $e(X,t)$ defined as $e := \frac{1-\phi_s}{\phi_s}$. The infiltration front $\delta(t)$ is a material boundary for the fluid phase and therefore travels with its own velocity $\mathbf{v}_f$. In the Lagrangian formulation

$$\frac{\mathrm{d}\delta}{\mathrm{d}t} = - \left.\frac{K(e_r+1)^2}{\mu\, e(e+1)}\frac{\partial P}{\partial X}\right|_{X=\delta}\,, \tag{2.4}$$

which can be obtained by writing Darcy's law (2.3.II) in coordinates fixed to the solid matrix at rest.

The following system of equations holds in the infiltrated (or wet) part of the preform, neglecting the inertia of the fluid

$$\begin{cases} \dfrac{\partial e}{\partial t} - (e_r+1)\dfrac{\partial v}{\partial X} = 0, \\ \dfrac{\rho_s}{e_r+1}\dfrac{\partial v}{\partial t} - \dfrac{\partial T}{\partial X} = -\dfrac{\partial P}{\partial X}, \end{cases} \qquad X \in [0,\ \delta(t)) \tag{2.5}$$

where $v = v(t,\ X)$ is the velocity of the solid preform, $T = T(e)$ is the stress in the preform. In the dry region, we have the following model

$$\begin{cases} \dfrac{\partial e}{\partial t} - (e_r+1)\dfrac{\partial v}{\partial X} = 0, \\ \dfrac{\rho_s}{e_r+1}\dfrac{\partial v}{\partial t} - \dfrac{\partial T}{\partial X} = 0. \end{cases} \qquad X \in [\delta(t),\ L] \tag{2.6}$$

Note that we use the same functional form of the excess stress tensor $T(e)$ for both the wet and the dry regions, thus assuming that the preform does not change its mechanical properties after being infiltrated.

A characteristic analysis of the hyperbolic systems of Equations (2.5) and (2.6) (see next Section) demonstrates that one boundary condition has to be supplemented at the solid borders and two continuity conditions (for flux of mass and momentum) at the infiltration front.

We suppose the preform to be relaxed at the initial time and the solid velocity to be zero. The position of the right border of the preform is fixed and therefore a Dirichlet boundary condition of zero displacement applies. The left one moves during the process and the condition to be imposed is the continuity between the normal stress of mixture and the applied load. This is not a trivial issue, as the stress in the mixture involves both the pressure of the mixture P and the excess stress T. A detailed discussion of this delicate issue is beyond the scope of this paper, we just refer the interested reader to the relevant literature ([13], [14]). In the present work we assume that the value of P matches at the boundary with the external fluid pressure [12] so that the excess stress is zero therein. This means that the left border presents a void ratio equal to the relaxed value. Again we assume the pressure to be continuous across the infiltration front and, neglecting the dynamics of the air in the dry region (which means $P = \text{const} = 0$ in the dry zone), see [15], we have

$$[[\rho_s \phi_s v\, \dot{\delta}]] - [[T]] = 0\,, \tag{2.7}$$

where $[[a]] = a(\delta^+) - a(\delta^-)$. The first difference in Equation (2.7) is very small in the problem under consideration, so that continuity of the excess stress across the infiltration front will be assumed. We shall consider again this point in the final section when discussing the numerical results.

The above considerations lead to the following set of initial and boundary conditions

$$\begin{cases} e(t=0,\ X) = e_r & \forall X \in [0,\ L] \\ v(t=0,\ X) = 0 & \forall X \in (0,\ L] \\ e(t,\ X=0) = e_r & \forall t \\ v(t,\ X=L) = 0 & \forall t \\ e(t,\ X=\delta^-) = e(t,\ X=\delta^+) & \forall t \\ v(t,\ X=\delta^-) = v(t,\ X=\delta^+) & \forall t, \end{cases} \tag{2.8}$$

where L is the initial length of the preform.

3. Approximate analysis of a pressure driven process

As argued in the literature (also based on numerical simulations, [8]), the effect of inertia in the applications is important only for a very short time interval (if compared to the overall infiltration time), during which the infiltrated region is very small (when compared to the total sponge length).

When inertia is neglected completely [15], the preform is suddenly compressed at a constant void ratio. If inertia is not neglected, the preform compresses at a finite (even if very large) velocity. The sudden initial compression determines the formation of traveling waves in the dry region, and the sponge starts to oscillate.

The system of Equations (2.6) does not account for any dissipation mechanisms in the dry sponge: dissipation occurs in the wet region only, due to the interactions between the infiltrating liquid and the sponge. Hence we expect the oscillations to decay in time.

In what follows we show that, under some simplifying assumptions, it is possible to capture some features of this complex phenomenon. We argue that the motion of the left solid border is essentially driven by two mechanisms: (1) the interaction of the wet region with the elastic waves traveling in the dry region; (2) the infiltration process.

We will study such phenomena separately, substituting the equations for the wet region with a very simple model. In Section 3.1 we study the onset of shocks and their influence on the motion of the left border, under the simplifying assumption that the wet region has a constant thickness δ: the wet region is modeled as a point mass whose dynamics is determined by the stress tensor at the infiltration front and the applied pressure. In Section 3.2 the wet region is considered in more detail: the enlargement of the wet region increases the mass $\rho_s \delta$ of the material point considered previously, yielding the decay of the oscillations; furthermore, dissipation occurs in the wet region, due to the relative velocity between the two phases.

3.1. Velocity of the left border of the preform during the initial compression

Assume in the following $\delta \ll L$. Integrating in space Equation (2.2.II) in the correponding domain, we obtain

$$\frac{\rho_s}{e_r + 1} \int_0^\delta \frac{\partial v}{\partial t} \, \mathrm{d}X = T(e_c(t)) + \Delta P \,, \tag{3.1}$$

where ΔP is the pressure drop externally applied at the whole system showing that the value of the void ratio at the infiltration front e_c is a function of time. Assuming $\frac{\partial v}{\partial t}$ to be constant in the small wet region, we can write

$$\rho_s \, \delta \left. \frac{\partial v}{\partial t} \right|_{X=\delta} = (e_r + 1)\,(T(e_c(t)) + \Delta P)\,. \tag{3.2}$$

Equation (3.2) gives a simplified model of the system: the wet region is studied as a point mass (with mass $\rho_s \delta$). Such a point mass is affected by two types of actions: a constant pressure gap and the response of the deformed matrix.

Now we estimate the response of the dry preform. Due to the compression, the absolute value of the excess stress in the dry region increases. A shock wave is generated which goes up and down through the dry zone giving rise to oscillations.

We can write the system of equations in the dry region (2.6) in the following matrix form

$$\frac{\partial \mathbf{u}}{\partial t} + \mathbf{A} \frac{\partial \mathbf{u}}{\partial X} \; = \; 0 \,,$$

where

$$\mathbf{u} = \begin{pmatrix} e \\ v \end{pmatrix}, \quad \mathbf{A} = \begin{pmatrix} 0 & e_r + 1 \\ \dfrac{e_r + 1}{\rho_s} T'(e) & 0 \end{pmatrix}. \tag{3.3}$$

Introducing Riemann invariants [16 pp. 291–300], we may rewrite the system (2.6) as follows

$$\frac{\partial z_1}{\partial t} - \lambda(\mathbf{u}) \frac{\partial z_1}{\partial X} = 0, \quad \frac{\partial z_2}{\partial t} + \lambda(\mathbf{u}) \frac{\partial z_2}{\partial X} = 0 \tag{3.4}$$

where z_1 and z_2 are the Riemann invariants, $\pm\lambda$ are the corresponding eigenvalues of the matrix **A**:

$$z_1 = (e_r + 1)\left(v + \int_0^e \sqrt{\frac{T'(\xi)}{\rho_s}}\,\mathrm{d}\xi\right), z_2 = (e_r + 1)\left(v - \int_0^e \sqrt{\frac{T'(\xi)}{\rho_s}}\,\mathrm{d}\xi\right),$$
$$\lambda = (e_r + 1)\sqrt{\frac{T'(e)}{\rho_s}}. \tag{3.5}$$

The first invariant z_1 is constant along the characteristics entering the (x, t) plane across the line $t = 0$. Remembering the initial conditions $e(t = 0,\ X) = e_r$ and $v(t = 0,\ X) = 0$, we have

$$v(t < \tau,\ X = \delta) = \int_e^{e_r} \sqrt{\frac{T'(\xi)}{\rho_s}}\,\mathrm{d}\xi\,, \tag{3.6}$$

where τ is the time taken by the characteristic line passing through $(t = 0,\ X = L)$ to reach the left border. From the previous equation we have a relation between the velocity and the void ratio on the left border. Such a relation can be inverted and substituted for the velocity in Equation (3.2). In this way, we obtain an equation for the velocity of the left solid border, which can be solved with the initial condition $v(t = 0,\ X = \delta) = 0$.

In the injection-molding process, the first compression is very rapid compared with the period of the oscillations; the void ratio reaches a value very close to $e_{c1} = T^{-1}(-\Delta P)$, so that the r.h.s. of Equation (3.2) is almost equal to zero and the velocity approximates a constant value $\overline{v}$. Hence, the void ratio along the dry preform can be approximated by a step function with jump $e_{c1} - e_r$. The shock propagates to the right side of the preform. Imposing there the boundary condition of zero velocity, and remembering that along the characteristics propagating to the right z_2 is constant (see Figure 2), we obtain the value of the void ratio at the right boundary in the following implicit form

$$\int_{e_{c2}}^{e_{c1}} \sqrt{\frac{T'(\xi)}{\rho_s}}\,\mathrm{d}\xi = \overline{v}\,. \tag{3.7}$$

The previous relation gives the value of the void ratio e_{c2} which travels back to the left border. Such a value is lower than e_{c1}, so that $T(e_{c2}) < -\Delta P$ and hence the left border is forced to invert its motion after the reflection of the second shock.

Iterating such a procedure we can study the oscillations of the border.

3.1.1. *The case of linear stress*

The simplest application can be studied when the stress depends linearly on the void ratio

$$T(e) = \Sigma(e - e_r)\,, \tag{3.8}$$

where Σ is a positive constant. The system of equations in the dry region reduces to

$$\frac{\partial e}{\partial t} - (e_r + 1)\frac{\partial v}{\partial X} = 0, \quad \frac{\rho_s}{e_r + 1}\frac{\partial v}{\partial t} - \Sigma\frac{\partial e}{\partial X} = 0\,. \tag{3.9}$$

The Riemann invariants and the modulus of the eigenvalues now simply read

$$z_1 = (e_r + 1)\left(v + \sqrt{\frac{\Sigma}{\rho_s}}\,e\right), z_2 = (e_r + 1)\left(v - \sqrt{\frac{\Sigma}{\rho_s}}\,e\right), \lambda = (e_r + 1)\sqrt{\frac{\Sigma}{\rho_s}}. \tag{3.10}$$

The problem now is linear and the speed of propagation of the discontinuities is equal to the eigenvalues. Following the same procedure of the previous section, when the infiltration starts we have

$$e(t,\ X=\delta) = e_r - \sqrt{\frac{\rho_s}{\Sigma}}v\,, \tag{3.11}$$

and, substituting in the equation for the wet region, we obtain

$$\delta\rho_s \frac{\partial v}{\partial t} = (e_r+1)(\Delta P - \sqrt{\Sigma\rho_s}v)\,, \tag{3.12}$$

whose solution is

$$v(t) = \frac{\Delta P}{\sqrt{\Sigma\rho_s}}(1 - \mathrm{e}^{-\frac{e_r+1}{\delta}\sqrt{\frac{\Sigma}{\rho_s}}t})\,. \tag{3.13}$$

For typical values of the process, the velocity reaches quickly the asymptotic value $v_{\max;0} = \frac{\Delta P}{\sqrt{\Sigma\rho_s}}$. In fact, we can say that the relaxation time is of the order of $\tau_r = \frac{\delta}{e_r+1}\sqrt{\frac{\rho_s}{\Sigma}}$, whereas the time of propagation along the dry region is $\tau = \frac{L-\delta}{\lambda} \cong \frac{L}{\lambda} = \frac{L}{e_r+1}\sqrt{\frac{\rho_s}{\Sigma}}$, so that we have $\frac{\tau_r}{\tau} = \frac{\delta}{L}$. Hence, the velocity of the sponge is a step function traveling towards the right border at a speed λ. From the previous expression for the void ratio at $X=0$, substituting $v \cong v_{\max;0}$ we have

$$e(t,\ X=\delta) \cong e_r - \frac{\Delta P}{\Sigma}\,. \tag{3.14}$$

At time $\tau \cong \frac{L}{\lambda}$, the traveling wave reaches the right border of the solid preform, where the solid velocity is zero. Imposing the Riemann invariant z_2 to be constant along the characteristics entering the domain in $X=\delta$, we obtain the value of the void ratio at $X = L$

$$\begin{aligned} e(t>\tau,\ X=L) &= e_r - 2\sqrt{\frac{\Sigma}{\rho_s}}v(t-\tau,\ X=0) \cong e_r - 2\sqrt{\frac{\Sigma}{\rho_s}}v_{\max;0} \\ &= e_r - 2\frac{\Delta P}{\Sigma}\,, \end{aligned} \tag{3.15}$$

where we consider the void ratio as a step function, neglecting again the relaxation time related to the velocity. Imposing z_1 to be constant along the characteristics coming back to the left solid border, we obtain

$$e_1(t,\ X=\delta) \cong e_r - 2\frac{\Delta P}{\Sigma} - \sqrt{\frac{\rho_s}{\Sigma}}\,v_1 \tag{3.16}$$

where the subscript 1 designates the quantities related to the coming back of the first traveling wave. Substituting the previous expressions, we obtain the following equation for v_1

$$\delta\rho_s \frac{\partial v_1}{\partial t} = (e_r+1)(-\Delta P - \sqrt{\Sigma\rho_s}v_1), \quad v_1(t=2\tau) = \frac{\Delta P}{\Sigma} \tag{3.17}$$

whose solution is

$$v_1(t') = -\frac{\Delta P}{\sqrt{\Sigma\rho_s}}(1 - 2\,\mathrm{e}^{-\frac{e_r+1}{\delta}\sqrt{\frac{\Sigma}{\rho_s}}t'})\,, \quad t' = t - 2\tau > 0\,. \tag{3.18}$$

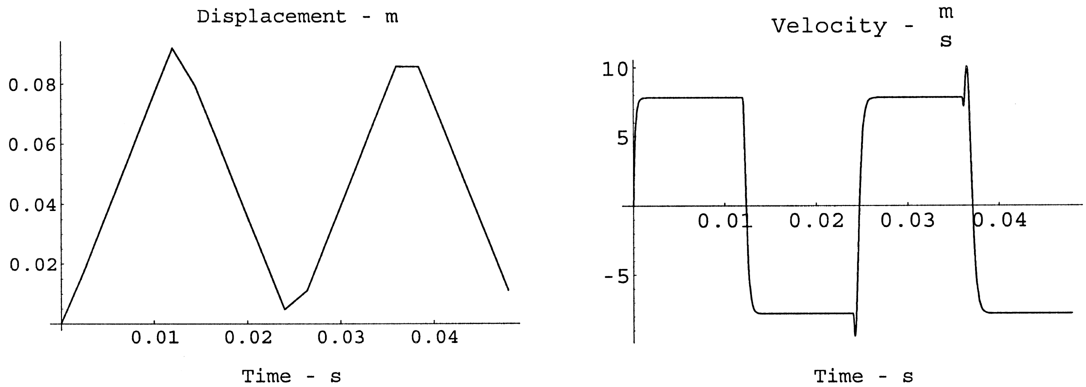

Figure 2. Velocity and displacement of the solid border.

We see again that the velocity reaches quickly (after a very short relaxation time, with the same relaxation time constant) a constant asymptotic value, which is $v_{\min;1} = -\frac{\Delta P}{\sqrt{\Sigma\rho_s}}$.

Proceeding now to the study of the waves traveling along the dry sponge, we see that the velocity of the left border is almost equal to a periodic step function with period $4\tau = 4\frac{L}{\lambda}$ and values $v_{\max;i} = \frac{\Delta P}{\sqrt{\Sigma\rho_s}}$ for i even, and $v_{\min;i} = -\frac{\Delta P}{\sqrt{\Sigma\rho_s}}$ for i odd.
Integrating over time such an approximation of the velocity, we obtain the following approximate expression for the motion of the left solid border

$$s(t) = \begin{cases} \dfrac{\Delta P}{\sqrt{\Sigma\rho_s}}t & \text{if } t \in \left[4i\tau,\ 2(2i+1)\tau\right) \\ \dfrac{\Delta P}{\Sigma}\dfrac{2L}{e_r+1} - \dfrac{\Delta P}{\sqrt{\Sigma\rho_s}}t & \text{if } t \in \left[2(2i+1)\tau,\ 4(i+1)\tau\right) \end{cases}, \tag{3.19}$$

where $i = 0, 1, 2, \ldots$. It is a triangular wave with period and amplitude given by

$$T = 4\tau = \frac{4L}{e_r+1}\sqrt{\frac{\rho_s}{\Sigma}}, \quad s_{\max} = \frac{2L}{e_r+1}\frac{\Delta P}{\Sigma}. \tag{3.20}$$

Also the void ratio, as a function of X, is almost equal to a step function: the value at the infiltration front is always equal (except for a relaxation time) to $e_r - \frac{\Delta P}{\Sigma}$ and the other constant (asymptotic) values traveling up and down the sponge are $e_r - 2\frac{\Delta P}{\Sigma}$ and e_r (the latter is obtained after the reflection on the right border when the velocity of the left border is negative; it is simple to verify, imposing z_2 to be constant along the characteristics emanating from the left border).

To compare this approximate solution, obtained by substituting the asymptotic values of the velocity $v_{\max;i}$ or $v_{\min;i}$, with the solution of the problem considering the time evolution of the velocity of the left border, we report in Figure 2 the result of a simple numerical routine which solves the equations discussed above without the approximation on the velocity. The corresponding values of the parameters will be presented in the following section. We can note that the relaxation time is very small.

3.2. Decay of the oscillations

The analysis of the section above accounts only for very early times when the thickness of the wet region δ does not vary appreciably. Furthermore, in the analysis presented in so far, there is no discussion on dissipation phenomena. The thickness of the infiltrated region is assumed to be constant in the time interval at hand, so that the 'force applied on the wet region' (which is modeled as a point mass) produces periodically the same effects. As the process of infiltration goes on, the wet region becomes larger and its thickness influences the oscillations of the left border of the preform. In what follows we remove the above assumption to explain how the motion of the infiltration front can contribute to the decay of the amplitude of the oscillations.

In the following three sections we will describe the evolution of the infiltration front, the effects on the motion of the sponge and the energy dissipation in the wet region.

3.2.1. *Evolution of the infiltration front*

To solve Equation (2.3) for the motion of the infiltration front δ, we need to relate the pressure gradient to δ. We can assume that the pressure in the infiltration region varies almost linearly and that its slope at the infiltration front could be approximated by the slope of the straight line taking the boundary values of the pressure on $x = 0$ and $x = \delta$. Hence, we recover the following equation

$$\frac{\mathrm{d}\delta}{\mathrm{d}t} \cong \frac{K(e_r+1)^2}{\mu\, e_c(e_c+1)}\frac{\Delta P}{\delta} = R[e_c]\frac{1}{\delta}\,. \tag{3.21}$$

Considering the case of linear stress tensor, we observe that the void ratio at the infiltration front (neglecting the relaxation times) takes the value:

$$e_c \cong e_r - \frac{\Delta P}{\Sigma}\,. \tag{3.22}$$

We can now consider $R[e_c]$ as a constant. This allows to solve analytically the equation for the infiltration front, obtaining

$$\delta(t) \cong \sqrt{2\,R[e_c]}\sqrt{t}\,. \tag{3.23}$$

Remark. We can note that, according to Equation (3.23), the infiltration boundary moves at an infinite velocity at $t = 0$. This paradox is related to the assumption that the inertia of the fluid is neglected; however, it is not negligible for small t. The complete conservation equation for the momentum of the fluid is given by the following equation which should substitute Equation (2.4)

$$\epsilon\frac{\mathrm{d}v_l}{\mathrm{d}t} + \frac{\mathrm{d}\delta}{\mathrm{d}t} = -\frac{K(e_r+1)^2}{\mu\, e(e+1)}\left.\frac{\partial P}{\partial X}\right|_{X=\delta}\,, \tag{2.4bis}$$

where $\epsilon = \frac{(1+e)^2}{e^2}\frac{K\rho_l}{\mu}$. When, during the initial infiltration, the solid velocity with respect to that of the fluid is neglected, Equation (2.4*bis*) can be written as a second-order equation for δ. For physical values of the parameters, $\epsilon \simeq 10^{-3}$, whereas $\frac{K(e_r+1)^2}{\mu\, e(e+1)}\Delta P \simeq 1$. Thus Equation (2.4bis) is a singular perturbation equation. The momentum term allows to satisfy one boundary condition more than Equation (3.21), which is that the velocity (not only the position) of the infiltration boundary vanishes at $t = 0$. The effect of the momentum of the fluid vanishes rapidly, converging to the asymptotic solution (3.23).

3.2.2. *Movement of the left border in the case of linear stress*

In the previous sections we always assumed the thickness of the infiltrated region δ to be small. As the infiltration process proceeds, we need to relax such an assumption. As a consequence some of the approximations considered above are not valid if the thickness of the infiltration region is not negligible: the velocity and the void ratio cannot be approximated by step functions. The relaxation times increase as the infiltration process proceeds. The effect is a deformation from a step function of the velocity of the left solid border as a function of time: such a deformation lasts for a time of the order of two times the relaxation time. As such a velocity is related to the formation of traveling waves in the dry region, its deformation produces a corresponding change in the shape of such waves.

In what follows, we provide an approximate study of this phenomenon, giving a qualitative discussion on the shape of the traveling waves in the dry region and a quantitative description of the velocity of the solid at the infiltration front. The better approximation of the velocity presented allows to obtain a more precise description of the oscillations, yielding a first justification of their decay.

Effects of the increasing of the wet region on the velocity of the left solid border. Similarly, as we obtained in the previous Section (3.1.1) for the application to the case of a linear stress tensor, assuming the thickness of the infiltrated region δ to be constant, the velocity of the left border of the sponge (with the exception of the first compression starting from $v(t = 0,\ X = 0) = 0$) is given by

$$v(t) = \pm\frac{\Delta P}{\sqrt{\Sigma\rho_s}}(1 - 2\,\mathrm{e}^{-\frac{e_r+1}{\delta}\sqrt{\frac{\Sigma}{\rho_s}}t})\,, \tag{3.24}$$

where the plus or minus sign refers to the reflection of an odd or even traveling wave, respectively, and the time $t = 0$ corresponds to the incidence on the left solid border of the wave considered. We can assume δ to be almost constant during the small time in which the velocity relaxes to the asymptotic value $\pm\frac{\Delta P}{\sqrt{\Sigma\rho_s}}$. This means that we can consider the previous expression as a good approximation for the velocity of the border, even if the infiltration is dependent on time.

Now, in order to study the decay of the amplitude of the oscillations, we consider δ to assume different (constant) values in each oscillation. For our simplified model, this means that the mass of the infiltrated region increases in time.

Integrating in time the expression of the velocity of the left border of the sponge, we obtain the following expression for the displacement of the border after the reflection of a traveling wave

$$s(t) = \pm\frac{\Delta P}{\sqrt{\Sigma\rho_s}}\,t \mp \frac{2\,\delta}{e_r + 1}\,\frac{\Delta P}{\Sigma}(1 - \mathrm{e}^{-\frac{e_r+1}{\delta}\sqrt{\frac{\Sigma}{\rho_s}}\,t}) + s_0\,, \tag{3.25}$$

where s_0 is the position of the border when the traveling wave arrives.

We can give an estimate of s_0 as follows: as the infiltrated region is large δ, the dry region is long $L-\delta$. Therefore the traveling wave reaches the infiltration front before the time estimated by the calculations yielding the triangular wave (3.19). We can estimate the correction in the decay of the oscillation due to the smaller extension of the dry region as

$$\Delta s_1 = \frac{\delta}{\Sigma}\frac{\Delta P}{e_r + 1}\,, \tag{3.26}$$

which is the distance covered by the oscillating border in the time taken by a traveling wave to cover δ.

Remark. The mass of the infiltrated region changes during an oscillation. Consider the time when the velocity of the solid at the infiltration front is $\frac{\Delta P}{\sqrt{\Sigma \rho_s}}$, the value for which the stress tensor $T(e_c)$ at the infiltration front is equal to the applied jump of pressure ΔP. As the force applied to the point mass modeling the wet region vanishes, its momentum $\rho_s \delta\, v$ must be conserved. Hence, we could expect that the velocity will reduce, as the mass $\rho_s \delta$ increases and the applied forces vanish. But, we should note that, as the velocity reduces, the void ratio at the infiltration front increases, reducing the stress, yielding a positive force $\Delta P + T(e_c)$ which increases the velocity. This means that a negative feedback stabilizes the velocity of the solid at the infiltration front, yielding a positive constant value until the wave traveling through the dry region returns.

Now we can return to Equation (3.25), in which an estimate of s_0 can be given. The reflection of the wave forces the left border to invert its motion, but, due to the inertia of the infiltrated region, the inversion is not sharp: for very small t, $\mathrm{e}^{-\frac{e_r+1}{\delta}\sqrt{\frac{\Sigma}{\rho_s}}\,t} \cong 1 - \frac{e_r+1}{\delta}\sqrt{\frac{\Sigma}{\rho_s}}\,t$ in Equation (3.25), yielding that the left border continues to compress the sponge initially. From Equation (3.24) we deduce that compression goes on untill the exponential term is equal to $\frac{1}{2}$ (which means that its exponent is almost equal to 0·7) and then the inversion of the motion starts. At such a time the oscillation reaches its maximum absolute value:

$$s_M \cong |s_0| + 0{\cdot}3 \frac{\delta}{e_r + 1} \frac{\Delta P}{\Sigma}\,. \tag{3.27}$$

This means that the amplitude of the oscillations reduces to $0{\cdot}7 \frac{\delta}{e_r+1} \frac{\Delta P}{\Sigma}$ at each reflection.

Deformation of the traveling waves. From the expressions (3.16) and (3.18) we have

$$e_1 = e_r - \frac{2\Delta P}{\Sigma} - \sqrt{\frac{\rho_s}{\Sigma}}\, v_1 = e_r - \frac{2\Delta P}{\Sigma} + \frac{\Delta P}{\Sigma}\left(1 - 2\,\mathrm{e}^{-\frac{e_r+1}{\delta}\sqrt{\frac{\Sigma}{\rho_s}}t}\right), \tag{3.28}$$

where we measured the time from the impinging of the traveling wave. We can note that for very small values of t we have an elongation; when the exponent of the exponential function in Equation (3.28) is equal to $\log \frac{1}{2} \cong 0{\cdot}7$, the void ratio is equal to $e_r - \frac{2\Delta P}{\Sigma}$, *i.e.*, the constant value of the traveling wave before the reflection; when it is larger than 3 the void ratio is almost equal to $e_r - \frac{\Delta P}{\Sigma}$ (with an error less than 10%), *i.e.*, the constant value of the traveling wave after the reflection.

Furthermore, we note that the exponent in the exponential is given by t times $\frac{e_r+1}{\delta}\sqrt{\frac{\Sigma}{\rho_s}}$, which is the inverse of the time taken by a wave to cover a length equal to δ. This means that, referring to that noted above, the deformation of the traveling wave has a length of $3\,\delta$ and presents a first sharp elongation vanishing at a distance $0{\cdot}7\delta$.

We can give a physical interpretation of the deformation of the shape of the reflected wave, focusing on our simplified model; let us consider the reflection of the first wave which impinges on the point mass which models the wet region (see Figure 3): as it has inertia, it does not change the velocity sharply, and for the first time it continues to present a positive velocity; as a consequence the solid matrix compresses, giving rise to the elongation described above; when the point mass inverts its motion, the matrix starts to relax.

Let us consider again the first reflection of a traveling wave. We can approximate its exponential expression with a step function, placing the jump at the average value of the exponential function, which means at a distance 2δ from the beginning of the elongation (recalling the relation $\int_0^\infty x\,\mathrm{e}^{-x}\mathrm{d}x = 2$). This can be interpreted as a delay time for the reflection of the traveling wave (approximated as a step function) equal to the time needed for a wave to go up and down the wet region.

The deformation of a wave traveling through the dry region after n oscillations is the sum of the deformations gained in the previous $2\,n$ reflections at the left border. We deduce that when large infiltration is considered and a great number of reflections has occurred, the void ratio in the dry region is far from the step function approximating it in the previous calculations. A better approximation can be given by two constant values connected by a straight line which gives a transition between such values in the region in which the deviation from a step function is great.

When the transition region has a length bigger than two times that of the dry region, the velocity of the left border does not reach any longer its maximum value $v_0 \cong \frac{\Delta P}{\sqrt{\Sigma\rho_s}}$, since the effect of a subsequent wave affects the left border before the energy of the previous one is completely transferred to the point mass modeling the wet region. This means that the velocity presents smooth oscillations with smaller maximum value. As the maximum value of velocity decreases, so does the maximum of the void ratio in the dry region. As a consequence a quick decay of the oscillations of the left border occurs.

Remark. As the traveling waves determine the solid velocity at the infiltration front we can give a qualitative description of the velocity of the solid matrix at the infiltration front during the first oscillations. As mentioned above, the void ratio after the first reflection is an exponential, presenting an elongation with respect to the step function and then a decay. The elongation is the first part of the wave coming back to impinge on the infiltration front. As a consequence, the velocity increases somewhat its absolute value when the wave reaches it. After this short period (of the order of $0{\cdot}7\frac{\delta}{\lambda}$), the velocity increases smoothly, and a new oscillation starts. In Figure 6 we show such an interesting elongation of the function velocity *vs.* time, which appears before the inversion of the motion of the wet region, from the reflection of the second wave (since the first one is a perfect step function).

3.2.3. *Energy associated with the oscillations*

Modeling the wet region as a point mass means neglecting the dynamics inside it. Indeed, we note that Equation (2.5.I) was not considered at all in the previous discussion and that we used Equation (3.2), which is an approximation of (2.5.II).

Therefore, phenomena like the relaxation of the matrix in the wet region or the oscillations occurring inside it have been neglected. This means that we are neglecting phenomena connected to the storing and restoring of mechanical energy in the wet region, supposing that the whole energy is the kinetic energy of the point mass modeling it.

In what follows we focus on the energy balance associated with the process under consideration.

Energy stored in the dry region. In terms of energy, we can say that the main features of the system can be captured by considering the transformation of the energy stored in the dry region into kinetic energy of the wet and dry regions. Let us then evaluate the energy stored in the matrix which allows the oscillations to occur. We can say that it is equal to the potential energy associated to the compressed dry region (which means a constant void ratio in the dry region equal to $e_c' = e_r - \frac{2\Delta P}{\Sigma}$) minus the amount of energy stored by the matrix at equilibrium, when the oscillations disappear (constant void ratio in the dry region equal to $e_c = e_r - \frac{\Delta P}{\Sigma}$). Hence we have the following potential energy

$$\int_{\delta}^{L} \Sigma(e_r - e_c')\,\mathrm{d}X - \int_{\delta}^{L} \Sigma(e_r - e_c)\,\mathrm{d}X \cong \Delta P(L - \delta)\,, \tag{3.29}$$

where unit cross-section area is assumed.

As the infiltration front advances, the energy stored in the dry region decreases and we see from Equation (3.29) that it is zero when the infiltration is fulfilled. In what follows we will discuss another contribution to the decay of the oscillations, given by the dissipation of kinetic energy in the wet region. To explain it we need to consider the full model of the wet region, remembering the physical meaning of each term.

Dissipation of energy in the wet region. In the wet region dissipation occurs due to the relative motion of the fluid and solid phases. Indeed, the thermal admissibility of the constitutive relations for the interaction terms forces the choice of the positive sign of the permeability and viscosity in Darcy's law and we will see in the following that a measure of the dissipation of kinetic energy is related to the relative velocities of the two phases and to their interactions, as modeled by Darcy's law.

Let us consider the problem written in the Eulerian formulation for the general three-dimensional case (the system of Equations (2.3)). Now we can multiply the first Equation (2.3.I) by the solid velocity $\mathbf{v}_s$, Equation (2.3.II) by the fluid velocity $\mathbf{v}_f$, and sum to obtain

$$\phi_s \rho_s \frac{\mathrm{d}}{\mathrm{d}t}\frac{v_s^2}{2} = -\frac{\mu\phi_f^2}{K}(\mathbf{v}_f - \mathbf{v}_s)^2 - \mathbf{v}_c \cdot \operatorname{grad} P + \mathbf{v}_s \cdot \operatorname{div}\mathbf{T}\,, \tag{3.30}$$

where $\mathbf{v}_c$ is the composite velocity. Let us now integrate in the part $\mathcal{B}(t)$ of the continuum that we are studying

$$\begin{aligned}\int_{\mathcal{B}(t)} \phi_s\rho_s \frac{\mathrm{d}}{\mathrm{d}t}\frac{v^2}{2}\,\mathrm{d}V &= \frac{\mathrm{d}}{\mathrm{d}t}\int_{\mathcal{B}(t)} \phi_s\rho_s \frac{v^2}{2}\,\mathrm{d}V \\ &= \int_{\mathcal{B}(t)} \left(-\frac{\mu\phi_f^2}{K}(\mathbf{v}_f - \mathbf{v}_s)^2 - \mathbf{v}_c \cdot \operatorname{grad} P + \mathbf{v}_s \cdot \operatorname{div}\mathbf{T}\right)\mathrm{d}V\,, \end{aligned} \tag{3.31}$$

where $\mathrm{d}V$ denotes an infinitesimal volume element. Integrating by parts in the r.h.s. we obtain

$$\begin{aligned}\frac{\mathrm{d}}{\mathrm{d}t}\int_{\mathcal{B}(t)} \phi_s\rho_s \frac{v^2}{2}\,\mathrm{d}V + \int_{\mathcal{B}(t)} \operatorname{tr}(\mathbf{T}\mathbf{D}_s)\,\mathrm{d}V &= -\int_{\mathcal{B}(t)} \frac{\mu\phi_f^2}{K}(\mathbf{v}_f - \mathbf{v}_s)^2\,\mathrm{d}V \\ &\quad - \int_{\partial\mathcal{B}(t)} \left(P\mathbf{v}_c + \mathbf{T}\mathbf{v}_s\right)\cdot \mathbf{n}\,\mathrm{d}S\,, \end{aligned} \tag{3.32}$$

where $\mathbf{D}_s = \operatorname{grad}\mathbf{v}_s$ is the stretching tensor of the solid matrix and $\operatorname{tr}(\mathbf{T}\mathbf{D}_s)$ is the stress power of the matrix. Hence the l.h.s. is the total energy of the wet portion $\mathcal{B}(t)$ of the mixture considered. The r.h.s. is given by two contributions: a surface and a volume term. The surface term is related to the energy supplied by the external world; the volume term is due to the local interactions between the two phases, and accounts for dissipation.

Let us now turn to the one-dimensional problem we are interested in. Let us consider $\mathcal{B}(t)$ to be the Eulerian counterpart of the wet region at a certain instant of time t (which means $[0,\ \delta(t)]$). As $\mathcal{B}(t)$ is composed of material points, we have to consider only the points reached by the fluid at time t, not those reached afterwards, as the infiltration continues. This means that we must subtract a convection term from the l.h.s. of (3.30)

$$\frac{\mathrm{d}}{\mathrm{d}t}\int_0^\delta \frac{\rho_s}{1+e_r}\,\frac{v^2}{2}\,\mathrm{d}X + \int_0^\delta T\,D\,\mathrm{d}X \;=\; \frac{\rho_s}{1+e_r}\,\frac{v^2}{2}\bigg|_\delta\,\frac{\mathrm{d}\delta}{\mathrm{d}t} - \Big[u_{\mathrm{in}}P + T\,v\Big]_0^\delta - \int_0^\delta \frac{\mu e^2}{K(1+e)(1+e_r)}(v_f - v)^2\,\mathrm{d}X\,, \tag{3.33}$$

where $D = \frac{\partial v}{\partial X}$ is the one dimensional Lagrangian counterpart of $\mathbf{D}_s$.

The first and second term in the r.h.s. of Equation (3.33) are surface contributions which correspond to the energy associated with the infiltration and with the oscillatory motion of the wet region (discussed in the previous section). The third term is a volume contribution representing the dissipation of energy in the wet region. Let us study such a term: substituting Darcy's law

$$V_f = \frac{1+e}{1+e_r}(v_f - v) = -\frac{K(e_r+1)^2}{\mu\,e(e+1)}\frac{\partial P}{\partial X}\,, \tag{3.34}$$

where V_f is the Lagrangian velocity of the fluid with respect to the solid, we can express the relative velocity in terms of the pressure gradient and obtain the following expression for the dissipation of energy $E(t)$ in the wet region due to the relative motion of the two phases

$$\begin{aligned} E(t) &= \int_0^t\int_0^\delta \frac{\mu e^2}{K(1+e)(1+e_r)}(v_f - v)^2\,\mathrm{d}X\,\mathrm{d}t \\ &= \frac{K}{\mu}\int_0^t\int_0^\delta \frac{(e_r+1)^5}{(e+1)^5}\left(\frac{\partial P}{\partial X}\right)^2\mathrm{d}X\,\mathrm{d}t\,. \end{aligned} \tag{3.35}$$

If we approximate the pressure gradient in the wet region as a constant equal to $\frac{\Delta P}{\delta}$ and the void ratio as equal to the average value $\overline{e} = e_r - \frac{\Delta P}{2\Sigma}$, we obtain[1]

$$E(t) \cong \frac{K}{\mu}\int_0^t \frac{(e_r+1)^5}{(\overline{e}+1)^5}\frac{\Delta P^{\,2}}{\delta}\,\mathrm{d}t \cong \frac{\sqrt{2}\,K}{\mu}\frac{(e_r+1)^5}{(\overline{e}+1)^5}\frac{\Delta P^{\,2}}{\sqrt{R[e_c]}}\sqrt{t}\,. \tag{3.36}$$

Now that we know how much of the energy is dissipated due to the interaction between the phases during infiltration, we can compare it with the energy stored in the matrix which allows the oscillations to occur. The time needed to dissipate all the energy that forces the solid matrix to oscillate can be obtained by requiring such energies to be equal

$$E(t^*) \cong \frac{\sqrt{2}\,K}{\mu}\frac{(e_r+1)^5}{(\overline{e}+1)^5}\frac{\Delta P^{\,2}}{\sqrt{R[e_c]}}\sqrt{t^*} = \Delta P(L - \sqrt{2R[e_c]\,t^*})\,. \tag{3.37}$$

From Equation (3.37) we have the following expression for the decay time

$$t^* = \beta\frac{\mu\,L^2}{2\,K\,\Delta P}\,, \tag{3.38}$$

[1] We remember that the left border of the solid matrix is relaxed and the infiltration front presents a void ratio equal to $e_r - \frac{\Delta P}{\Sigma}$, except for the transition periods in which a wave traveling in the dry region is reflected.

Table 1. Numerical values of the physical parameters.

Variable	Value	Measure unit
ρ_s	2530	Kg/m^3
Σ	$1{\cdot}6 \times 10^6$	J/m^2
K	$2{\cdot}53 \times 10^{-9}$	m^2
e_r	1	
ΔP	5×10^5	Pa
μ	0·135	Pa·s
L	0·3	m

where

$$\beta = \frac{\dfrac{(e_r+1)^2}{e_c(e_c+1)}}{\left(\dfrac{(e_r+1)^5}{(\overline{e}+1)^5} + \dfrac{(e_r+1)^2}{e_c(e_c+1)}\right)^2}\,. \tag{3.39}$$

If we want to evaluate the time in which the energy dissipated is of a certain amount, for example we want to evaluate the time for which the system has dissipated α times the initial energy (with $\alpha < 1$), we have the same expression for t^* but with β substituted by

$$\beta_1 = \frac{\dfrac{(e_r+1)^2}{e_c(e_c+1)}}{\left(\dfrac{1}{\alpha}\dfrac{(e_r+1)^5}{(\overline{e}+1)^5} + \dfrac{(e_r+1)^2}{e_c(e_c+1)}\right)^2}\,. \tag{3.40}$$

4. Comparison with numerical simulations

The full problem illustrated in Section 2 can be solved numerically in the Eulerian formulation by a Godunov-type scheme [8, 17], using a moving grid which can possibly be remeshed. All the parameters used in the simulation of the model are specified in Table 1.

Such parameters are approximations of the experimental data reported in the following, which refer to the infiltration of a thermosetting resin in a network of glass fibers, neglecting the curing [18]:

– the viscosity corresponds to the expression for the viscosity of the resin [19, 20]

$$\mu\,(\Theta,\,\delta_c) \;=\; \bar{\mu}\;\exp\left(\frac{E_\mu}{R\,\Theta}\right) \tag{4.1}$$

(where R is the gas constant, $E_\mu = 18000$ J/mole is the activation energy) evaluated for a temperature of 350 K

– the stress tensor is the secant between e_r and e_c^w for the stress-strain relation extrapolated by the data, reported in [21]

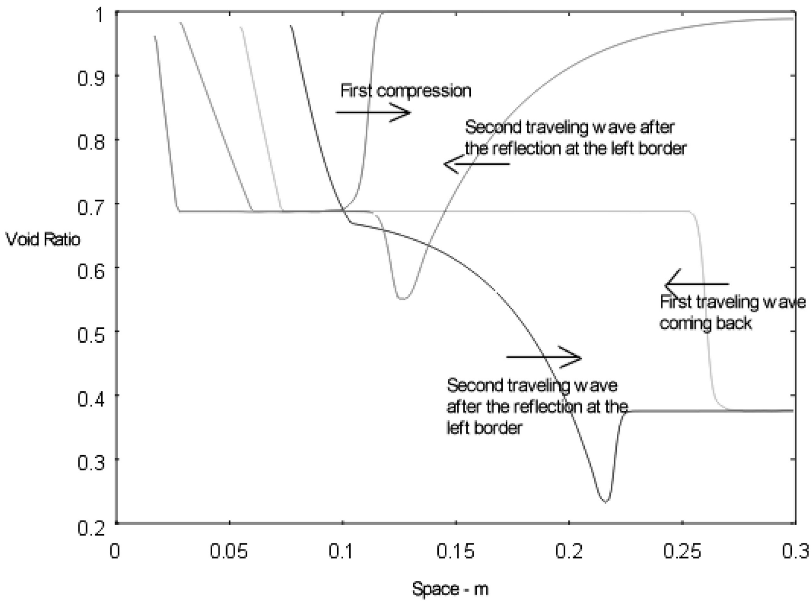

Figure 3. Traveling waves.

$$T' \;=\; \beta(\mathrm{e}^{\gamma\phi} - \mathrm{e}^{\gamma\phi_r})\,, \tag{4.2}$$

where $\beta = 0{\cdot}09$ Pa and $\gamma = 26{\cdot}4$

– the permeability is assumed to depend explicitly only on the porosity and, referring to [22], we use the following relation

$$K(\phi_s) \;=\; K_0\mathrm{e}^{\alpha(\phi_1-\phi_s)}, \tag{4.3}$$

evaluated at the mean value between e_r and e_c^w.

In Figure 3 we can see the void ratio as a function of X at four different instants of time: the wave travels up and down the dry region twice, and the graphs are related to the void ratio after the first compression and the following three reflections. The void ratios predicted for the reflections are

$$e_0 = e_r = 1, \quad e_1 = e_r - \frac{\Delta P}{\Sigma} \cong 0{\cdot}69, \quad e_2 = e_r - 2\frac{\Delta P}{\Sigma} \cong 0{\cdot}38, \quad e_3 = e_r\,. \tag{4.4}$$

In Figure 3 we can also note the deformation of the second traveling wave with respect to the first one: the wave traveling for the first time is a perfect step function, the second one presents an elongation ($0{\cdot}7X_i$ long, *i.e.* of the order of 0·03 m at the first reflection) and an exponential decay (with characteristic length of the order of X_i), as described in the previous section.

In Figure 4 the first oscillations of the left border of the matrix are reported, which are to be compared with the amplitude and the frequency obtained analytically. The period of the oscillations predicted theoretically is

$$T = \frac{4L}{e_r+1}\sqrt{\frac{\rho_s}{\Sigma}} \cong 0{\cdot}024\,\mathrm{s}\,, \tag{4.5}$$

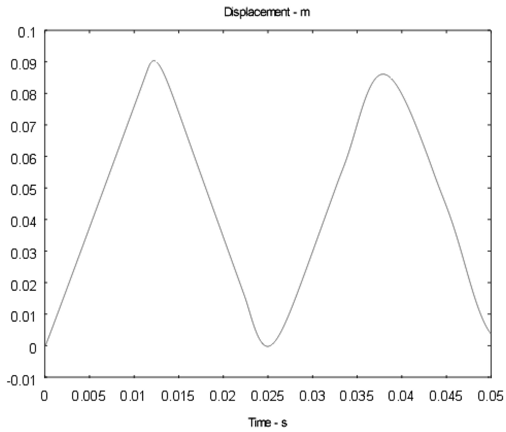

Figure 4. First oscillations of the left border.

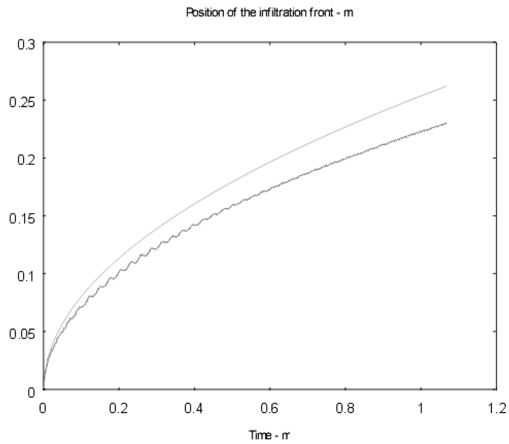

Figure 5. Position of the infiltration front: comparison between the full model (black line) and the reduced one (grey line).

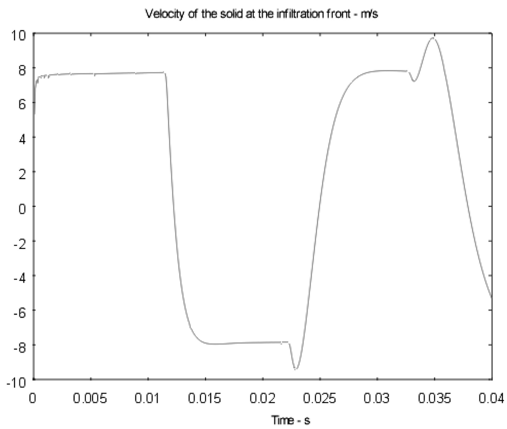

Figure 6. Velocity of the solid at the infiltration front as a function of time.

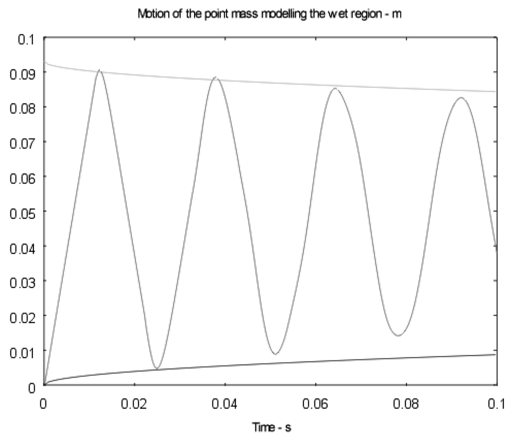

Figure 7. Decay of the oscillations: the two functions delimiting the oscillations refer to the predicted decay.

and the amplitude is

$$s_{\max} = \frac{2\,L}{e_r + 1}\,\frac{\Delta P}{\Sigma} \cong 0{\cdot}093\,\mathrm{m}\,. \tag{4.6}$$

In Figure 5 the position of the infiltration front is shown, and a comparison with the approximate analytical result, in the Eulerian framework. We note that the numerical simulations start with a finite infiltrated region of 1 mm.

Figure 6 shows the velocity of the solid at the infiltration front. As noted in the previous section an elongation appears, from the second reflection of a traveling wave, due to the inertia

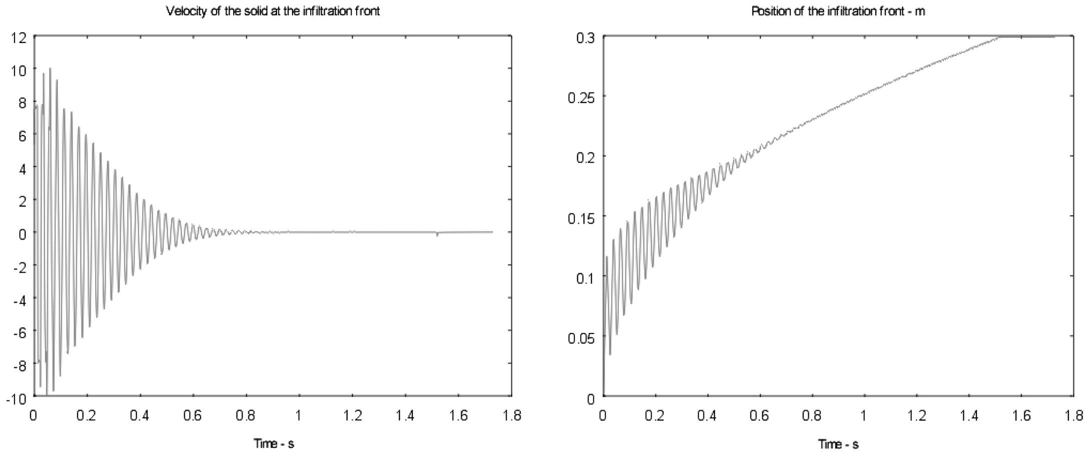

Figure 8. Infiltration process for a long time of infiltration: the figure on the left shows the velocity of the solid at the infiltration front as a function of time; the figure on the right shows the position of the infiltration front in the Eulerian framework.

of the wet region which produces a further compression of the preform before the inversion of the motion of the point mass that models the wet region.

We can now discuss the approximation introduced in Equation (2.4) in the light of the numerical simulations. The velocity of the solid at the infiltration front is of the order of 6 m/s; the infiltration velocity, except for the very early time, is less then 10 m/s. This means that the jump of momentum across the infiltration front is at most 10% of the jump of the stress. This is largely an overestimation, as is confirmed by the numerical simulations, which do not predict any jump across the infiltration front.

In Figure 7 the decay of the oscillations is shown. The motion is evaluated by integrating the velocity of the solid at the infiltration front (all our results are for such a velocity). It is worth noticing that it does not correspond to the motion of a material point; if we want to study the motion of the left solid border, we also have to take into account its relaxation, which, referring to [12], can be evaluated by

$$v_{lsb} = \left. \frac{K}{\mu} \frac{\partial T'_w}{\partial \phi} \frac{\partial \phi}{\partial x} \right|_{x=x_i} - \left. \frac{K}{\mu} \frac{\partial T'_w}{\partial \phi} \frac{\partial \phi}{\partial x} \right|_{x=x_e}, \tag{4.7}$$

where x_i and x_e are the Eulerian positions of the infiltration front and the left solid border, respectively.

In Figure 7 we also show the functions $0{\cdot}7 \frac{X_i}{e_r+1} \frac{\Delta P}{\Sigma}$ and $s_{\max} - 0{\cdot}7 \frac{X_i}{e_r+1} \frac{\Delta P}{\Sigma}$ that model the decay due to the increase of the mass of the point mass modelling the wet region (see Section (3.2.2)), but neglecting the energy dissipation in the wet region. We can see that the approximation of the decay is good only for the first oscillations.

Finally, in Figure 8 two simulations are presented that allow us to determine the time in which the oscillations of the wet region disappear: the first graph shows the velocity of the solid at the infiltration front as a function of time for a long process time; the second graph presents the position of the infiltration front in the Eulerian framework. We can see that the oscillations in the velocity disappear in 0·8 seconds, but the energy associated with such oscillations is strongly reduced before that time. The time for the full dissipation of the energy predicted by the discussion of Section (3.2.3) is

$$t^* = \beta \frac{\mu L^2}{2K \Delta P} = 0{\cdot}68\,\text{s}. \tag{4.8}$$

The time needed to dissipate 75% of the energy is

$$t^* = \beta_1 \frac{\mu L^2}{2K \Delta P} = 0{\cdot}56\,\text{s}. \tag{4.9}$$

5. Final remarks

A model for of the infiltration of an incompressible liquid through a solid porous medium has been introduced, in the framework of mixture theory. The model has been applied for typical conditions characterizing industrial processes involving injection molding through an elastic preform, when a constant pressure on the injected fluid is applied.

By some simplifying assumptions, an analytical discussion is given for the case of a linear stress tensor, focusing on the role of inertial terms. Some qualitative features of the phenomenon have been studied: the decay of such oscillations in the early stages of the infiltration process in terms of the parameters entering the system (permeability, stress, the sponge solid phase, applied pressure gap); estimates for the displacement of the infiltration front have been derived. These estimates compare well with the results obtained by a numerical simulation of the complete model.

References

1. J. Bear, *Hydraulics of groundwater.* New York: McGraw–Hill (1979) 450 pp.
2. R. De Boer, Theory of porous media: past and present *ZAMM* 78 (1998) 441–466.
3. M.A. Biot, General theory of three-dimensional consolidation. *J. Appl. Phys.* 12 (1941) 155–164 .
4. M.A. Biot, Theory of elasticity and consolidation for a porous anisotropic solid. *J. Appl. Phys.* 26 (1955) 182–185.
5. M.A. Biot, Theory of deformation of a porous anisotropic solid. *J. Appl. Phys.* 27 (1956) 459–464.
6. M.A. Biot, A theory of finite deformations of porous solid. *Indiana Univ. Math. J.* 21 (1972) 597.
7. C. Truesdell, Sulle basi della termodinamica, Rendiconti dell’Accademia dei Lincei, XXII, 33–38 (1957) 158–166.
8. D. Ambrosi and L. Preziosi, Modeling injection molding processes with deformable porous preforms. *SIAM J. Appl. Math.* 61 (2000) 22–42.
9. D. Antonelli and A. Farina, Resin transfer moulding: mathematical modelling and numerical simulation. *Composites A* 30 (1999) 1367–1385.
10. K. Wilmanski, *Thermo-Mechanics of Continua.* Berlin/Heidelberg: Springer (1998) 284 pp.
11. K. Wilmanski, Lagrangean model of two-phase porous material. *J. Non-Equil. Thermodyn.* 20 (1995) 50–77.
12. L. Preziosi and A. Farina, Deformable porous media and composites manufacturing. In: K. Markov and L. Preziosi (eds.), *Heterogeneous Media.* Boston: Birkhauser (2000) pp. 321–410.
13. I.S. Liu, On chemical potential and incompressible porous media. *J. de Mécanique* 19 (1980) 327–342.
14. W. Jager and A. Mikelic, On the interface boundary condition of Beavers. Joseph and Saffman. *SIAM J. Appl. Math.* 60 (2000) 1111–1127.
15. D. Ambrosi, Infiltration through deformable porous media. *ZAMM* 82 (2002) 115–124.
16. P. Bassanini and A.R. Elcrat, *Theory and Applications of Partial Differential Equation.* New York and London: Plenum Press (1997) 450 pp.

17. E. Lacoste, O. Mantaux and M. Danis, Numerical simulation of metal matrix composites and polymer matrix composites processing by infiltration: a review. *Composites A* 33 (2002) 1605–1614.
18. R. Larsson, M. Wysocki and S. Toll, Process-modeling of composites using two-phase porous media theory. *Eur. J. Mech. - A/Solids* 23 (2004) 15–36.
19. M.R. Kamal and S. Sourour, Kinetics and thermal characterization of thermoset cure. *Polymer Eng. Sci.* 13 (1973) 59–64 .
20. S. Sourour and M.R. Kamal, Differential scanning calorimetry of epoxy cure: isothermal cure kinetics. *Thermodyn. Acta* 14 (1976) 41–59.
21. Y.R. Kim, S.P. McCarthy and J.P. Fanucci, Compressibility and relaxation of fiber reinforcements during composite processing. *Polymer Compos.* 12 (1991) 13–19.
22. W.B. Young, K. Rupel, K. Han, L.J. Lee and M.J. Liou, Analysis of resin injection moulding in molds with preplaced fiber mats. II: Numerical simulations and experiments of mold filling. *Polymer Compos.* 12 (1991) 30–38.